Study of neurovascular coupling by modulating neuronal activity with GABA

Harsha Radhakrishnan[*], **Weicheng Wu**, **David Boas**, and **Maria Angela Franceschini**
Photon Migration Imaging Laboratory, MGH/MIT/HMS Athinoula A. Martinos Center for Biomedical Imaging, Massachusetts General Hospital/Harvard Medical School, USA

Abstract

Fundamental to the interpretation of neurovascular coupling is determining the neuronal activity that accounts for functional hyperemia. Recently, synaptic and not spiking activity has been found to be responsible for the hemodynamic response. Using pharmacological manipulation in rats, we want to further determine whether the cortical synaptic activity generated by the thalamic input or the subsequent synaptic activity related to secondary cortical processing is driving the hemodynamic response. In this study, we topically applied γ-aminobutyric acid (GABA) in the somatosensory cortex and used electrical forepaw stimulation to evoke neural and vascular activity. In a group of 8 animals, using laminar electrophysiology, we verified that topical application of GABA for 20 min does not affect layer IV synaptic activity but reduces subsequent activity in the supragranular and infragranular layers. In another group of 8 animals, we simultaneously measured the electrical and vascular responses with scalp electroencephalography (EEG) and diffuse optical imaging (DOI), respectively. We decomposed somatosensory evoked potentials (SEP) into three major components: P1, N1, and P2, where P1 represents the thalamic input activity originating in layer IV, and N1 and P2 represent the subsequent cortical transmissions. We verified that GABA infusion in the somatosensory cortex does not significantly reduce the P1 SEP component but strongly reduces the N1 and P2 components. We found GABA also elicits a large reduction in the hemodynamic responses, which correlate with the reduction in N1 and P2 components. These results suggest that the hemodynamic response is predominantly driven by cortico-cortical interactions and not by the initial thalamocortical activity in layer IV.

Keywords

Neurovascular Coupling; GABA; Diffuse Optical Imaging; Near Infra-Red Spectroscopy; EEG; Somatosensory Evoked Potentials

---

Research highlights

- Infusing GABA on the cortex reduces the supragranular layer sink but not the initial sink in layer 4.

---

[*]Corresponding author: Harsha Radhakrishnan, Athinoula A. Martinos Center for Biomedical Imaging, Massachusetts General Hospital, 149, 13th street, Rm 2277, Charlestown, MA 02129. Phone : (617) 726-9332, Fax : 617) 643-5136, harsha@nmr.mgh.harvard.edu.

- Correlated reductions in hemodynamic response and N1 and P2 SEP components are seen with GABA.

- Cortico-cortical interactions and not initial layer IV activity drives the hemodynamic response.

1. Introduction

Functional studies of the human brain are performed either by measuring electrical activity with electroencephalography (EEG) and magnetoencephalography (MEG) or by measuring the vascular responses with functional magnetic resonance imaging (fMRI), positron emission tomography (PET) and diffuse optical imaging (DOI). While we know that alterations in neural activity and metabolism correlate with changes in cerebral blood flow (CBF) and cerebral blood volume (CBV), it is still not clear what mechanisms link these processes. Given the growing role of fMRI and DOI in neuroscience, quantifying the relationship between the hemoglobin signal and the underlying neural activity is becoming increasingly important. Most efforts have involved invasive measurements in animals using microelectrodes and various optical microscopy imaging methods, yielding information fundamental to understanding the relationship between electrophysiological and hemodynamic evoked responses (Ngai et al., 1998; Ureshi et al., 2004). In particular, recent studies have shown that functional hyperemia depends more on synaptic and postsynaptic activity than on spiking activity (Logothetis and Wandell, 2004; Mathiesen et al., 1998; Rauch et al., 2008; Viswanathan and Freeman, 2007). In the majority of neurovascular coupling studies to date, either the whole synaptic activity or the initial afferent inputs are considered, under the common assumption that it is the initial cortical activity in layer IV that drives the hemodynamic response (Iadecola, 2004 as a review). In previous studies (Franceschini et al., 2008; Franceschini et al., 2010), we observed that there is better correlation between the hemodynamic response and secondary and late neuronal activity than with the principal activity in layer IV. In agreement with this initial finding, Angenstein et al. (Angenstein et al., 2009) have recently shown how the input cortical activity alone is not able to justify the hemodynamic response behavior and hypothesized the involvement of further cortical processing.

In this study, we want to address this issue more directly, by measuring electrical and vascular responses while pharmacologically altering secondary and late activity and preserving thalamic input and layer IV initial cortical activity. To reduce the neuronal activity of the most superficial cortical layers, we topically infuse the surface of the rat brain with γ-aminobutyric acid (GABA). GABA widely hyperpolarizes cortical neurons, thus reducing synaptic and spiking activity (Kyriazi et al., 1996). GABA penetrates very slowly from the surface into deep cortical layers (Roberts et al., 1980), and in the first 30–40 min after application does not affect the principal activity in layers IV (Brailowsky and Knight, 1984; Staba et al., 2004). In a group of animals, using laminar electrophysiology and applying GABA in the cortical surface, we verify we reduce neural activity in superficial layers, without significantly affecting neural activity in layer IV.

Similar to our previous work (Franceschini et al., 2008; Franceschini et al., 2010), to measure electrical and vascular functional responses in a second group of animals we combine two macroscopic noninvasive techniques: electroencephalography (EEG) and diffuse optical imaging (DOI). These measurements offer a bridge between the findings from invasive microscopic techniques and noninvasive macroscopic measurements, furthering our understanding of neurovascular coupling. Both techniques measure a large volume of tissue and, while they offer poor spatial resolution, are sensitive to changes in all

cortical layers. In particular, with EEG we can distinguish initial layer IV and subsequent activity by decomposing the somatosensory evoked potentials (SEP) into three or four components. Activation of the somatosensory cortex by a discrete peripheral stimulus generates four SEP components: P1, N1, P2 and N2. The relationship of these surface components to local field potentials (LFP) and neural activity has been studied extensively in the past 30 years and is mostly established (Jellema et al., 2004; Mitzdorf, 1985). The surface P1 SEP component corresponds to the primary evoked potential and arises from synaptic excitation of middle layers activated by specific thalamocortical inputs (Agmon and Connors, 1991; Simons, 1978). During P1, a current sink appears in layers IV and V and a corresponding current source appears in superficial cortical layers (Amassian et al., 1964; Li et al., 1956; Mitzdorf, 1985). Following this initial depolarization, axon-collaterals of layer Vb pyramidal cells produce an enhanced activation of the supragranular pyramidal cells in layer I–II, which generates the secondary surface evoked potential N1 (Agmon and Connors, 1991; Jellema et al., 2004; Kulics and Cauller, 1986). During N1, a large sink appears in layers I and II and one or two sources appear in layers III and V (Kulics and Cauller, 1986). P2 and N2 arise from activation of cortico-cortical connections originating in the superficial layers (Kulics and Cauller, 1986; Wrobel et al., 1998) and derive from a combination of both inhibitory and repolarization processes (Steriade, 1984). The functional significance of these late SEP components is unclear due to inconsistent source-sink patterns and the absence of multi-unit activity (MUA) during this time (Kulics and Cauller, 1986). These studies have shown the link between different synaptic activities and the major SEP components. In this work we use these SEP components to determine which part of the synaptic activity is responsible for the hemodynamic response.

2. Results

In a group of 8 animals, we used laminar electrophysiology in the center of the forepaw somatosensory representation during contralateral forepaw electrical stimulation to measure local field potential (LFP), multi unit activity (MUA) in different cortical layers before and after topical application of 0.1 mM concentration of GABA in artificial cerebrospinal fluid (aCSF). The stimulation consisted of 14 four seconds trains of twelve 200-μs and <2 mA pulses delivered with hypodermic needles inserted into the forepaw. From the depth-resolved LFP, current source density (CSD) profiles were calculated using the software developed by A. Dale et al. (Pettersen et al., 2006). Fig. 1 shows the CSD profile in a representative animal. Blue and red curves represent data obtained before and 16–24 minutes after GABA application, respectively. The initial sink (negative deflection) in layer IV and corresponding source (positive deflection) in the surface is not affected by GABA application, while the sink in the supragranular layers and the corresponding source in the infragranular layers are reduced, similar to the findings reported by Staba (Staba et al., 2004). Fig. 2 reports the LFP, MUA and CSD profiles in specific cortical layers obtained by averaging over eight animals. In each animal, we normalized the signals with respect to the initial peak in layer IV in the cycles before GABA application. Error bars shown at every 10 ms represent standard errors. While we did not observe significant changes in MUA, possibly due to the small concentration of GABA used here and the relatively short time we waited after GABA application, the LFP activity significantly changed in superficial, supragranular and infragranular layers. The small change in amplitude observed in the LFP in the granular layer does not reach statistical significance (p-value>0.05).

Laser Doppler during the laminar electrophysiology experiments and diffuse correlation spectroscopy (DCS) during DOI/EEG experiments were used to monitor whether the infusion of GABA increased the baseline blood flow. In both LD and DCS measurements, the changes in blood flow between pre-infusion and GABA cycles were not statistically

significant (p-value > 0.1) and not correlated with the hemoglobin concentration changes during these conditions.

In 8 animals we did simultaneous EEG/DOI measurements. In each animal we performed 11 measurement cycles: 2 before, 2 during, and 2 after infusion of aCSF and after a 20 minute period, 1 before, 2 during, and 2 after infusion of 0.1 mM GABA dissolved in aCSF (Fig. 7, in the Methods Section). For each cycle, there were 2 minutes of DCS acquisition during rest, DOI and EEG acquisition of 14 electrical stimulation trains of the right forepaw (paw contralateral to infusion side, left SI), 2 min of DOI and EEG acquisition during 7 stimulation trains of the left forepaw (paw ipsilateral to the infusion side, right SI - control side). The data presented here are responses to contralateral stimulation only. Data represented as 'infusion side' refers to response from the left SI to right forepaw stimulation and data represented as 'control side' refers to response from the right SI to left forepaw stimulation.

In all our experiments we verified that the animal systemic blood pressure and heart rate did not change significantly when infusing the cortex with 0.1 mM of GABA. For the DOI/EEG group, systemic blood pressure values were 118 ± 11 mmHg, 121 ± 17 mmHg, and 119 ± 5 mmHg during pre-infusion, aCSF and GABA infusions, respectively. The respiration rate and body temperature were maintained at 44 ± 1 bpm and 37 °C, respectively. The average values of the blood-gas analysis across all experiments were: pH = 7.36 ± 0.01, pCO_2 = 36.2 ± 5.7 mmHg, and pO_2 = 192.9 ± 12 mmHg.

From the EEG data, for each cycle, we calculated the average SEP responses averaging both across trains and across stimuli. Fig. 3 shows the grand averaged EEG responses across rats for the infusion side (panels a and b) and the control side (panels c and d) during contralateral forepaw stimulations normalized with respect to the maximum amplitude of P1. Panels a and c report mean responses during pre-infusion, aCSF and GABA infusion cycles (averages of the last infusion cycle and two post-infusion cycles) with error bars (standard errors) shown every 5 ms. Panels b and d report the responses for each cycle with error bars shown every 10 ms. As stated earlier, the EEG responses were broken down into individual SEP components – P1, N1, and P2. In the infusion side, the N1 and P2 SEP components (both peak amplitude and area under the curve) are significantly reduced with GABA with respect to the cycles before GABA infusion. P1 peak amplitude is also reduced by GABA, but to a lower extent than N1 and P2.

Fig. 4 shows the hemodynamic changes measured in the somatosensory cortex in response to contralateral forepaw stimulation averaged across rats for the infusion (panels a and b) and the control (panels c and d) sides. Oxy-hemoglobin concentration (HbO) changes are positive, and deoxy-hemoglobin (HbR) changes are negative. Similar to Fig. 3, in Fig. 4, panels a and c report the mean responses for pre-infusion, aCSF and GABA cycles (averages of the last infusion cycle and two post-infusion cycles) and panels b and d report the responses for each cycle. Error bars representing standard errors are shown every 1 second. Both HbO and HbR are significantly reduced with GABA with respect to the cycles before GABA infusion.

Table I report the average percent changes of the area and the peak amplitudes of SEP and hemoglobin responses In the infusion side, while all quantities decreased in amplitude with GABA, P1 component become broader with GABA, so that the area under the curve of P1 did not change sufficiently with respect to the pre-infusion runs. As a result, reductions of ΣP1 were not statistically significant, while reductions of ΣN1, ΣP2, ΣHbO and ΣHbR with GABA were large and highly significant (p-values $\leq$0.002). Similarly, peak amplitudes of responses were also compared. Reductions in N1 and P2 were very close to reductions in

HbO and HbR. Changes in P1 peak amplitude were less significant and smaller than changes in N1 and P2. In the control side, we did not observe any statistically significant reduction on the area or peak amplitude of N1, P2, HbO and HbR during GABA and aCSF cycles, but we observed a statistically significant reduction of P1 peak amplitude and area during the GABA cycles. Finally we compared the SEP and hemodynamic responses in the two hemispheres before infusion (pre-infusion cycles) and did not observe any statistically significant difference in the responses due to the surgery in the infusion side.

The scatter plots in Fig. 5 show the correlation between the areas under the SEP components and the oxy-hemoglobin response curves for individual rats for the 11 cycles in the infusion side. A highly statistically significant correlation is achieved between either ΣN1 or ΣP2 and ΣHbO (see p-values in the figure) or ΣHbR (not shown for brevity). When comparing peak amplitudes, there is an improved correlation between P1 peak and hemodynamic response, but it is still statistically lower than correlations using N1 and P2 peak amplitudes.

Fig. 6 shows the hemoglobin responses measured and predicted by a linear convolution model (Franceschini et al., 2008) using the three SEP components, the total SEP signal T, and the input stimuli (S) for the grand average over all animals in the infusion side during pre-infusion, aCSF and GABA stages. To compare results, we calculated the coefficients of determination (R^2) between the measured and predicted hemoglobin concentrations. Using area under the SEP components as inputs to the model, over the 11 cycles, the R^2 values between the measured and predicted hemoglobin responses are 0.51–0.53 for P1 and input stimuli S, 0.65–0.67 for N1 and P2 for either HbO or HbR. The R^2 values of N1, P2 and T are statistically significantly larger than the R^2 obtained with P1 or S (p-value<0.02). Similarly, using the peak responses as inputs to the model (figure not shown), P1 has a statistically significant lower R^2 than N1 (p-values < 0.02). The P2 SEP component is very broad and does not have a well-defined peak, and even if it predicts hemodynamic responses better than P1, it does not reach statistical significance (p-value = 0.09). For the control side, we found predictions were similar for the different SEP components without statistically significant differences. The coefficients of determinations ranged between 0.54 to 0.61 for HbO and 0.59–0.64 for HbR. This underlies the fact there is no variance in the control side during the experiment because of the single stimulation condition used and lack of effect of GABA on the non-infused side. Finally, while the predictions for deoxy-hemoglobin were higher than for oxy-hemoglobin, they did not reach statistical significance.

3. Discussion

The main result of this study is that the hemodynamic response seems to follow secondary and late cortical activity more than the principal activity in layer IV. In the majority of neurovascular coupling studies to date, parametric stimulation is used to modulate neuronal activity. In the past, only a few studies have modulated the synaptic activity pharmacologically and measured the modified electrical and vascular responses simultaneously (Caesar et al., 2008; Caesar et al., 2003; Hoffmeyer et al., 2007; Kocharyan et al., 2007; Leithner et al., 2010; Shi et al., 2008). The advantage of pharmacological studies is that the modulation can be targeted to specific groups of neurons or specific cortical layers. This allows not only to establish a correlation between electrical and vascular responses but also to more directly determine cause and effect. Here, by targeting neural activity in superficial cortical layers, we determined their predominant involvement in driving hemodynamic response. This can be seen in the scatter plots in Fig. 5, where layer IV activity (P1) poorly correlates with the hemodynamic responses because GABA does not strongly affect P1 while the hemodynamic responses are significantly reduced by it. Subsequent electrical activity, N1 and P2, is more significantly affected by GABA and highly correlate with hemodynamic response. Predictions of hemodynamic response using

P1 (Fig. 6) are very similar to predictions using input stimuli, and suggest the role of the thalamic afferent activity is limited to trigger the hemodynamic response whose magnitude is then mediated by cortical transmissions.

Using laminar electrophysiology we first verified the penetration depth of GABA in the cortical layers. After cortical surface application of GABA for 16–24 min, we verified that neuronal excitation is reduced in the superficial cortical layers without significantly affecting the thalamic input synaptic activity in layer IV (Fig. 2). This is because GABA penetrates very slowly (tens of minutes) into deeper cortical layers. Roberts et al. (Roberts et al., 1980) reported an exponential decay of GABA uptake with a 50% concentration reduction at a depth of 200 μm after a 10 min exposure. The CSD profiles in Figs. 1 and 2 show that, after ~20 min application of GABA, the secondary sink in supragranular layers is reduced (p-value=0.02), while the initial sink in layer IV is not affected (p-value >0.05). This is in agreement with previous electrophysiology results (Brailowsky and Knight, 1984;Staba et al., 2004). Also, we did not observe significant changes in multiunit activity, confirming that in the 20 min of application GABA does not reach layers III and IV, where MUA originates. The laminar electrophysiology measurements support our EEG findings. The fact that N1 and P2 SEP components are strongly attenuated with GABA, while P1 is not significantly affected, is consistent with the significant attenuation of surface negative LFP and superficial CSD sink with GABA and its insignificant effect on the LFP and CSD sink in the granular layer.

Fig. 4 shows that the hemodynamic responses start to decrease before N1 and P2. One possible explanation is that the hemodynamic response is non-linearly related to the electrical activity (Devor et al., 2003;Hoffmeyer et al., 2007;Jones et al., 2004;Martindale et al., 2005;Norup Nielsen and Lauritzen, 2001;Sheth et al., 2004). We therefore tested a quadratic convolution model based on a simplification of the quadratic approach of Ances et al. (Ances et al., 2000) but found no improvement in the model prediction of the hemodynamic response. Another possible explanation is the diffusion time lag of the GABA from the cortical surface to the neuronal populations in layer II. It can take more than 10 minutes for GABA to diffuse to a depth of 200 μm (Roberts et al., 1980;Roy and Contreras, 2007), and affect the EEG signal, which is dominated by pyramidal neurons' currents (Mitzdorf, 1985). During this time, the N1 and P2 signals are not attenuated by GABA, but GABA's superficial presence could inhibit superficial cortical cells and consequently reduce evoked vascular responses in the upstream pial vessels. This would result in our observation of a reduced hemodynamic response without a reduction in N1 or P2 during the first 6 minutes, followed by reduction of N1 and P2 and further reduction of the hemodynamic response after 10 minutes when GABA starts to reach layer II. This is an important observation requiring further investigation with invasive measurements.

It was important to verify that baseline CBF did not change with infusing GABA (Fergus and Lee, 1997; Hamel, 2006), to confirm that the reductions in the hemodynamics was not a result of increased baseline blood flow. This is the reason we used lower concentrations of GABA than Staba et al. (Staba et al., 2004) and did not observe significant reduction in MUA during laminar electrophysiology experiments. With the concentration of GABA used here, we did not measure significant changes in baseline CBF (p-values > 0.1), or systemic blood pressure with GABA with respect to pre-infusion values. This is in agreement with previous publications that show preserved vascular reactivity and no changes in basal CBF during infusion of GABA and muscimol (Caesar et al., 2003; Kocharyan et al., 2007).

We also tested the effect of infusion of aCSF alone on the electrical and vascular responses and verified that infusion of aCSF alone in our closed scalp preparation for DOI/EEG measurements did not cause significant changes in the SEP and hemoglobin responses.

It was found that the N1 and P2 SEP components and the hemodynamic responses in the control side remained mostly constant throughout the experiment. The small variation of the electrical and vascular responses in the control side indicates that the animals were stable throughout the experiment and did not suffer from any physiological deterioration during the course of the measurement, which is also verified by the results of the blood-gas analyses and other physiological monitoring. In addition, the fact that N1 P2 and vascular responses in the control side do not change with GABA implies that the infusion is quite local.

It is interesting to note that there were small yet significant changes in P1 in the control side during GABA infusion while we did not observe a statistically significant change in P1 area in the infusion side with GABA. This may be due to the counterbalance effects of GABA that tends to increase P1 (Caesar et al., 2003; Staba et al., 2004) and neuronal habituation that decreases P1 (as in the control side). The small changes in LFP responses in the granular layer and the above mentioned changes in P1 in the control side are not due to any effects of GABA infusion. Although they exhibit some changes, it is evident from the scatter plots (Fig. 5) and the prediction analysis (Fig. 6) that they do not correlate well with the associated hemodynamic changes.

We estimate that, at a source-detector separation of 3.5 mm, DOI is sensitive to hemodynamic response changes of up to 2–3 mm below the skin. While DOI lacks the resolution needed to determine the cortical layer in which the hemodynamic signal originates, in rats, with this probe geometry, we can measure contributions to the hemodynamic response integrated over all cortical layers (Culver et al., 2003b). Several researchers have attempted to determine the laminar distribution of the hemodynamic responses, and, while not conclusive, their results suggest a similar magnitude of responses in the middle and superficial cortical layers (Gerrits et al., 2000; Hillman, 2007; Silva and Koretsky, 2002). And while with DOI we cannot discriminate hemoglobin contributions in depth, it is unlikely that the strong attenuation in hemodynamic response we observe with GABA is limited to a reduction in the superficial layers only. Further studies using methodologies with better z-resolution, such as MRI or optical coherence tomography will be able to verify this issue.

In conclusion, using macroscopic electrical and vascular measurements and modulating superficial neuronal activity with GABA, we were able to determine that the hemodynamic response better reflect the secondary activity in the superficial cortical layers than the initial synaptic activity in layer IV. With these measurements, we cannot rule out a reduction of the hemodynamic response in deeper cortical layers due to a reduction of neuronal activity in corresponding deeper layers subsequent to the decreased superficial neuronal activity.

4. Materials and Methods

4.1 Animal Preparation

Sixteen male Sprague Dawley rats were included in this study. Eight animals (319 ± 30 g) where used for the EEG/DOI neurovascular coupling experiments, and eight additional animals (271 ± 13 g) were measured with laminar electrophysiology to verify the effect of GABA on LFP at different cortical depths. During all surgical procedures the animals were anesthetized with isoflurane (2–2.5% v/v). After tracheotomy and cannulation of the femoral artery and femoral vein, the animal was mounted on a stereotactic frame. Heating blankets maintained core temperature at 36.5–37.5°C. For the EEG/DOI measurements, to topically infuse GABA in the cortex, a 1 mm^2 hole was drilled through the skull overlying the left SI, the underlying dura mater was removed with care, and a polyethylene tube (ID=0.28 mm, OD = 0.61 mm) inserted in the hole. Tissue adhesive was used to glue the catheter to the skull and the tissue above the craniotomy area was sutured back in place. To minimize

differences in intracranial pressure, ventriculostomy immediately under the occipital bone was performed allowing draining of excess cerebrospinal fluid during infusion. Craniotomy was also performed above the left somatosensory cortex (SI) on the eight animals used to measure neuronal activity by laminar electrophysiology. In this case, a well of dental cement was built around the exposed cortex to be filled with artificial cerebrospinal fluid solution (aCSF, pH = 7.4, KCl 5mM, NaCl 125mM, $C_6H_{12}O_6$ 10mM, $CaCl_2$ 3mM, and $MgCl_2$ 1mM, Sigma Aldrich, MO, USA) with and without GABA. Ventriculostomy was also done on these animals to keep the same prep as in the EEG/DOI group. The only difference between the two animal groups is that in the laminar electrophysiology group the cortex is exposed, while in the DOI/EEG group the exposed cortex area is sealed back during measurements. This difference is dictated by the different measurement modalities and may cause some differences on how fast the GABA penetrates the cortex.

Following the surgical procedures, the anesthesia was changed to alpha-chloralose (loading dose of 30 mg/kg and maintaining dose of 40 mg/kg/hr). To minimize transition effects, functional activation studies were performed after ~1 hour waiting period (Austin et al., 2005). Continuous monitoring of arterial blood pressure (MABP), tail artery oxygen saturation and heart rate, and blood samples recording of arterial pH, pO_2, and p_aCO_2 during various stages of the experiment, assured maintenance of basic physiological parameters. All procedures were approved by the Massachusetts General Hospital Subcommittee on Research Animal Care.

4.2. Measurement protocol

For the non-invasive experiments, after pre-infusion cycles we continuously infused the cortex for 16 minutes with a solution of aCSF alone, or with a 0.1 mM concentration of GABA (Sigma Aldrich, MO, USA) dissolved in the aCSF solution, at a rate of 0.02 ml/hour. We used the same catheter for the aCSF and GABA infusions. To avoid leakage, the catheter was glued to the skull. The infusion rate needed to be very slow to avoid increases of intracranial pressure and possible brain damage. The catheter was initially filled with aCSF solution and during the 16 min of aCSF infusion; the aCSF solution was replaced by the GABA solution from the syringe-pump. The length of the catheter (18 cm) was such that at our injection rate it took 16 min to fully replace the aCSF with GABA in the catheter. With this setup it is possible that a small amount of GABA may have reached the cortex before the end of the aCSF infusion.

In these experiments electrical stimuli were applied using hypodermic needles inserted into the left and right forepaws of the animals. The stimulation consisted of 4 seconds trains of twelve 200-μs pulses delivered at 3 Hz repetition rate as in (Franceschini et al., 2010). The amplitude of the stimuli was adjusted just above motor threshold by increasing the stimulation current until the forepaw movement was visible (1.3±0.3 mA range of current used). The stimuli were presented pseudo-randomly by randomizing the duration of the rest periods between trains. The average inter-stimulus interval (ISI) was 12 s (the ISI ranged from 2 to 20 s). For each cycle, 14 stimulation trains were applied to the right paw and 7 trains to the left paw.

For the invasive electrophysiology experiments, we waited 30 minutes after insertion of the laminar electrode for stable neuronal activity to return. Functional measurements were done, first with the cortex in a bath of aCSF alone (2 cycles), and then by replacing the aCSF with a solution of 0.1mM of GABA dissolved in aCSF (2 or 3 cycles). The stimulation paradigm timing was maintained similar to that of the DOI/EEG measurements. We acquired four minutes of data during the contralateral paw stimulation while the ipsilateral stimulation of the DOI/EEG measurements was replaced by a period of 4 minutes of rest for the animal.

4.3. Laminar electrophysiology recordings

LFP and MUA in different cortical layers were obtained using a linear multi-electrode array with 23 contacts spaced at 100 microns (Devor et al., 2003; Devor et al., 2008). The laminar electrode was inserted in the center of the left forepaw sensory representation contralateral to right forepaw electrical stimulation, identified by cortical mapping using a ball electrode made from silver wire (Warner Instruments, Hamden CT, USA). An Ag/AgCl reference electrode was placed subcutaneously in the neck.

The electrophysiology signals from the 23 channels of the laminar electrode were amplified and filtered between 500 and 5000 Hz to record MUA, and between 0.1Hz and 10 kHz to record LFP. For each animal, we averaged all stimuli in a run and identified layer IV responses as the earliest LFP negative deflection and the earliest CSD sink. To average all animals together, in each animal we identified the surface (depth 0–100 μm), supragranular layers (depth 200–400 μm), layer IV (depth 600–900 μm), and infragranular layers (1300–1600 μm). In each animal, we then normalized the signals with respect to the initial peak in layer IV in the cycles before GABA application. Comparisons and t-test statistical analysis are done between the pre-GABA cycles and second or third GABA cycles.

4.4. EEG recordings

The EEG data was obtained using a 40-channel monopolar digital amplifier system (NuAmps, NeuroScan, USA), as in (Franceschini et al., 2008). Four Ag/Agcl disk-type EEG electrodes (4 mm diameter, Warner Instruments, Hamden CT, USA) were used to record the neuronal activity and were placed around the optical probe under the animal skin (see Fig. 7). A ground electrode (8 mm diameter) was positioned above the nose of the animal and a 10 mm diameter reference electrode was positioned on the neck of the animal. Two ECG electrodes, 10 mm in diameter, were positioned on the torso of the animal, on the left and right sides, and an additional ground electrode was positioned more posterior in the animal torso. We used paste to keep the ground, reference and ECG electrodes in position. We verified that the impedance of the electrodes was smaller than 5KΩ. We verified that the cross talk between the stimulation and recording systems did not affect the features calculated from the EEG signals. The EEG and ECG measurements were carried out at a sampling frequency of 1 kHz.

For each animal, for either the infusion or the control side, the EEG data from the electrode in the contralateral SI cortex was high-pass filtered at a −3dB cutoff frequency of 3.5 Hz. A notch filter was applied to suppress 60 Hz interference and the ECG signal was used to reduce the arterial pulsation with a linear regression model. The three SEP components were isolated by evaluating the zero crossings of the SEP signal. The N2 component is negligible in our data because of the effect of the maintaining anesthetic used (Franceschini et al., 2010). In the cases where the SEP responses were small because of attenuation by GABA we used the zero crossings determined in the previous cycles. We normalized the signals for each animal by the maximum P1 response and then calculated the areas under the curve of each SEP component for each stimulus within a train for each cycle.

4.5. Diffuse optical imaging

DOI is a noninvasive technique that has been used for more than a decade to measure brain activity in humans (Hoshi and Tamura, 1993; Villringer et al., 1993). The technique quantifies local cortical hemodynamic changes spectroscopically by measuring light absorbance changes at different wavelengths, and has been extensively validated against fMRI (Huppert et al., 2006a; Huppert et al., 2006b; Kleinschmidt et al., 1996; Strangman et al., 2002; Toronov et al., 2001). For the measurements reported here, we used a continuous-wave imaging system (CW4, TechEn Inc., Milford, MA) as described in (Franceschini et al.,

2008; Siegel et al., 2003). In this system, eighteen laser diodes (nine emitting light at 690 nm, and nine at 830 nm) are frequency-encoded and their signals acquired simultaneously by sixteen parallel APD detectors. Each detector's output is digitized at 40 kHz. The individual source signals are filtered off-line by using an infinite-impulse-response filter with a 20 Hz bandpass frequency, which allows for a 10 Hz acquisition rate per image. The optical probe is comprised of a 4×4 grid of 16 detectors interleaved with a 3×3 grid of 9 sources (each source included a 690 and a 830 nm laser), and covers a flat region of the rat head extending 7.5 mm either side of the midline, and from 4 mm anterior to 11 mm posterior of the Bregma as shown in Fig. 7. Thirty-six source-detector pairs at a 3.5 mm separation (nearest neighbors) were considered for the data analysis. The optical probe was secured in contact with the head and supported by metal posts. The CW4 system used here is the same as we typically use in human experiments but the source-detector separations used in the animal experiments is 10 times smaller (Franceschini et al., 2003). In a previous work, we verified that the hemoglobin response measured with this system and probe in rats is co-localized and temporally equivalent to the BOLD response measured with fMRI (Culver et al., 2003b; Siegel et al., 2003). In particular, while here we did not attempt to resolve the hemodynamic responses in depth, but limited our study to the channels with the largest hemodynamic responses, Culver (Culver et al., 2003b) showed a good agreement between the depth of the hemoglobin responses measured with DOI and BOLD fMRI, demonstrating the ability of DOI to measure hemodynamic responses in both superficial and deeper somatosensory cortical layers.

Similar to the EEG data analysis, the DOI raw data for each animal, for either the infusion or the control side, were band-pass filtered between 0.02 and 0.5 Hz. Oxy- and deoxy-hemoglobin concentrations (HbO and HbR, respectively) were calculated using the modified Beer-Lambert law (Delpy et al., 1988) without any path-length correction. To obtain the average hemodynamic response for the 11 activation cycles, the data were deconvolved with the stimulation onsets. In each rat and on each side, we identified the source-detector pair with the most statistically significant oxy-hemoglobin activation in the contralateral SI cortex (p-value < 0.05) and used it for further data analysis. Before calculating the grand average across animals, HbO and HbR responses for each rat were normalized by the maximum HbO response during the 11 cycles in the same manner as for the SEP responses.

4.6. Measure of baseline cerebral blood flow

GABA at high concentrations acts as a vasodilator (Alborch et al., 1984; Lai et al., 1988). For this reason, we used a very low concentration (0.1mM) and in all of our measurements verified that local baseline blood flow was not affected (Kocharyan et al., 2007). A Laser Doppler probe (Periflux System 5000, Perimed, Sweden) was used in the invasive laminar electrophysiology experiments, while for the non-invasive EEG/DOI measurements we used a relatively new optical technique, diffuse correlation spectroscopy (DCS) (Cheung et al., 2001; Durduran et al., 2004a; Durduran et al., 2004b). The DCS instrument we used is similar to the system developed by Dr. Arjun Yodh at the University of Pennsylvania (Boas et al., 1995) and tested in several animal (Cheung et al., 2001; Culver et al., 2003a; Durduran et al., 2004b) and human experiments (Durduran et al., 2005; Durduran et al., 2004b; Yu et al., 2005). Our DCS system employs a solid-state long coherence length laser (785 nm, ~70 mW of power) to illuminate the surface of the head and four photon-counting avalanche photodiodes connected to four single-mode optical fibers to collect the diffusely reflected light. The intensity auto-correlation function of each channel is computed by a digital correlator. This four-channel system acquires one data point every second and the blood flow index is obtained off-line by fitting the measured electric field autocorrelation functions with a model of dynamic light scattering in deep tissues (Roche-Labarbe et al., 2010). We co-localized the source and 4 detector DCS fibers with the DOI fibers in the left

SI (infusion side) (Fig. 7). With the DCS, we measured the intensity auto-correlation function during the initial 2 minutes of rest at the beginning of each measurement cycle and we fit the data to a correlation diffusion model (Cheung et al., 2001) to obtain a blood flow index. We performed DCS measurements in 6 of the 8 EEG/DOI animals and laser Doppler measurements on 6 of the 8 laminar electrophysiology animals. For two animals in each group, the instruments were not available. While with laser Doppler we are sensitive to blood flow only in the superficial cortical layer, with the DCS, similar to DOI, we are sensitive to blood flow in both superficial and deeper layers (Carp et al., 2010).

4.7 Prediction of hemodynamic response using the different SEP components

We predicted the hemodynamic response for each cycle with a linear convolution model, as described in (Franceschini et al., 2008), using the area under the curve of the three SEP components (ΣP1, ΣN1 and ΣP2), the sum of the three components (ΣT), and the input stimuli (S) as inputs to the model. For all experiments, the temporal length of the convolution model was set to 10 s, which corresponded to 100 time samples. To compare results, we calculated the coefficients of determination (R^2) between the measured and predicted hemoglobin concentrations. We used Fisher's Z transform to map the bounded R^2 values into unbounded Z values, which better satisfy the assumption of normality, and performed a two-tailed paired t-test for significant differences in the Z transformed R^2 values for different SEP components.

Acknowledgments

References

Agmon A, Connors BW. Thalamocortical responses of mouse somatosensory (barrel) cortex in vitro. Neuroscience 1991;41:365–379. [PubMed: 1870696]

Alborch E, Torregrosa G, Terrasa JC, Estrada C. GABA receptors mediate cerebral vasodilation in the unanesthetized goat. Brain Res 1984;321:103–110. [PubMed: 6093926]

Amassian VE, Waller HJ, Macy J Jr. Neural Mechanism Of The Primary Somatosensory Evoked Potential. Ann N Y Acad Sci 1964;112:5–32. [PubMed: 14188115]

Ances BM, Zarahn E, Greenberg JH, Detre JA. Coupling of neural activation to blood flow in the somatosensory cortex of rats is time-intensity separable, but not linear. J Cereb Blood Flow Metab 2000;20:921–930. [PubMed: 10894175]

Angenstein F, Kammerer E, Scheich H. The BOLD response in the rat hippocampus depends rather on local processing of signals than on the input or output activity. A combined functional MRI and electrophysiological study. J Neurosci 2009;29:2428–2439. [PubMed: 19244518]

Austin VC, Blamire AM, Allers KA, Sharp T, Styles P, Matthews PM, Sibson NR. Confounding effects of anesthesia on functional activation in rodent brain: a study of halothane and alpha-chloralose anesthesia. NeuroImage 2005;24:92–100. [PubMed: 15588600]

Boas DA, Campbell LE, Yodh AG. Scattering and Imaging with Diffusing Temporal Field Correlations. Phys Rev Lett 1995;75:1855–1858. [PubMed: 10060408]

Brailowsky S, Knight RT. Inhibitory modulation of cat somatosensory cortex: a pharmacological study. Brain Res 1984;322:310–315. [PubMed: 6509318]

Caesar K, Offenhauser N, Lauritzen M. Gamma-aminobutyric acid modulates local brain oxygen consumption and blood flow in rat cerebellar cortex. J Cereb Blood Flow Metab 2008;28:906–915. [PubMed: 18000512]

Caesar K, Thomsen K, Lauritzen M. Dissociation of spikes, synaptic activity, and activity-dependent increments in rat cerebellar blood flow by tonic synaptic inhibition. Proc Natl Acad Sci U S A 2003;100:16000–16005. [PubMed: 14673091]

Carp SA, Dai GP, Boas DA, Franceschini MA, Kim YR. Validation of diffuse correlation spectroscopy measurements of rodent cerebral blood flow with simultaneous arterial spin labeling MRI; towards MRI-optical continuous cerebral metabolic monitoring. Biomed Opt Exp 2010;1:553–565.

Cheung C, Culver JP, Takahashi K, Greenberg JH, Yodh AG. In vivo cerebrovascular measurement combining diffuse near-infrared absorption and correlation spectroscopies. Phys Med Biol 2001;46:2053–2065. [PubMed: 11512610]

Culver JP, Durduran T, Cheung C, Furuya D, Greenberg JH, Yodh AG. Diffuse optical measurement of hemoglobin and cerebral blood flow in rat brain during hypercapnia, hypoxia and cardiac arrest. Adv Exp Med Biol 2003a;510:293–297. [PubMed: 12580443]

Culver JP, Siegel AM, Stott JJ, Boas DA. Volumetric diffuse optical tomography of brain activity. Opt Lett 2003b;28:2061–2063. [PubMed: 14587815]

Devor A, Dunn AK, Andermann ML, Ulbert I, Boas DA, Dale AM. Coupling of total hemoglobin concentration, oxygenation, and neural activity in rat somatosensory cortex. Neuron 2003;39:353–359. [PubMed: 12873390]

Devor A, Hillman EM, Tian P, Waeber C, Teng IC, Ruvinskaya L, Shalinsky MH, Zhu H, Haslinger RH, Narayanan SN, Ulbert I, Dunn AK, Lo EH, Rosen BR, Dale AM, Kleinfeld D, Boas DA. Stimulus-induced changes in blood flow and 2-deoxyglucose uptake dissociate in ipsilateral somatosensory cortex. J Neurosci 2008;28:14347–14357. [PubMed: 19118167]

Durduran T, Burnett MG, Yu G, Zhou C, Furuya D, Yodh AG, Detre JA, Greenberg JH. Spatiotemporal quantification of cerebral blood flow during functional activation in rat somatosensory cortex using laser-speckle flowmetry. J Cereb Blood Flow Metab 2004a;24:518–525. [PubMed: 15129183]

Durduran T, Choe R, Yu G, Zhou C, Tchou JC, Czerniecki BJ, Yodh AG. Diffuse optical measurement of blood flow in breast tumors. Opt Lett 2005;30:2915–2917. [PubMed: 16279468]

Durduran T, Yu G, Burnett MG, Detre JA, Greenberg JH, Wang J, Zhou C, Yodh AG. Diffuse optical measurement of blood flow, blood oxygenation, and metabolism in a human brain during sensorimotor cortex activation. Opt Lett 2004b;29:1766–1768. [PubMed: 15352363]

Fergus A, Lee KS. GABAergic regulation of cerebral microvascular tone in the rat. J Cereb Blood Flow Metab 1997;17:992–1003. [PubMed: 9307613]

Franceschini MA, Fantini S, Thompson JH, Culver JP, Boas DA. Hemodynamic evoked response of the sensorimotor cortex measured noninvasively with near-infrared optical imaging. Psychophysiology 2003;40:548–560. [PubMed: 14570163]

Franceschini MA, Nissila I, Wu W, Diamond SG, Bonmassar G, Boas DA. Coupling between somatosensory evoked potentials and hemodynamic response in the rat. NeuroImage 2008;41:189–203. [PubMed: 18420425]

Franceschini MA, Radhakrishnan H, Thakur K, Wu W, Ruvinskaya S, Carp S, Boas DA. The effect of different anesthetics on neurovascular coupling. NeuroImage 2010;51:1367–1377. [PubMed: 20350606]

Gerrits RJ, Raczynski C, Greene AS, Stein EA. Regional cerebral blood flow responses to variable frequency whisker stimulation: an autoradiographic analysis. Brain Res 2000;864:205–212. [PubMed: 10802027]

Hamel E. Perivascular nerves and the regulation of cerebrovascular tone. J Appl Physiol 2006;100:1059–1064. [PubMed: 16467392]

Hillman EM. Optical brain imaging in vivo: techniques and applications from animal to man. J Biomed Opt 2007;12:051402. [PubMed: 17994863]

Hoffmeyer HW, Enager P, Thomsen KJ, Lauritzen MJ. Nonlinear neurovascular coupling in rat sensory cortex by activation of transcallosal fibers. J Cereb Blood Flow Metab 2007;27:575–587. [PubMed: 16896350]

Hoshi Y, Tamura M. Detection of dynamic changes in cerebral oxygenation coupled to neuronal function during mental work in man. Neuroscience Letters 1993;150:5–8. [PubMed: 8469403]

Huppert TJ, Hoge RD, Dale AM, Franceschini MA, Boas DA. Quantitative spatial comparison of diffuse optical imaging with blood oxygen level-dependent and arterial spin labeling-based functional magnetic resonance imaging. J Biomed Opt 2006a;11:064018. [PubMed: 17212541]

Huppert TJ, Hoge RD, Diamond SG, Franceschini MA, Boas DA. A temporal comparison of BOLD, ASL, and NIRS hemodynamic responses to motor stimuli in adult humans. NeuroImage 2006b; 29:368–382. [PubMed: 16303317]

Iadecola C. Neurovascular regulation in the normal brain and in Alzheimer's disease. Nat Rev Neurosci 2004;5:347–360. [PubMed: 15100718]

Jellema T, Brunia CH, Wadman WJ. Sequential activation of microcircuits underlying somatosensory-evoked potentials in rat neocortex. Neuroscience 2004;129:283–295. [PubMed: 15501587]

Jones M, Hewson-Stoate N, Martindale J, Redgrave P, Mayhew J. Nonlinear coupling of neural activity and CBF in rodent barrel cortex. NeuroImage 2004;22:956–965. [PubMed: 15193627]

Kleinschmidt A, Obrig H, Requardt M, Merboldt KD, Dirnagl U, Villringer A, Frahm J. Simultaneous recording of cerebral blood oxygenation changes during human brain activation by magnetic resonance imaging and near-infrared spectroscopy. J Cereb Blood Flow Metab 1996;16:817–826. [PubMed: 8784226]

Kocharyan A, Fernandes P, Tong XK, Vaucher E, Hamel E. Specific subtypes of cortical GABA interneurons contribute to the neurovascular coupling response to basal forebrain stimulation. J Cereb Blood Flow Metab. 2007

Kulics AT, Cauller LJ. Cerebral cortical somatosensory evoked responses, multiple unit activity and current source-densities: their interrelationships and significance to somatic sensation as revealed by stimulation of the awake monkey's hand. Exp Brain Res 1986;62:46–60. [PubMed: 3956637]

Kyriazi HT, Carvell GE, Brumberg JC, Simons DJ. Quantitative effects of GABA and bicuculline methiodide on receptive field properties of neurons in real and simulated whisker barrels. J Neurophysiol 1996;75:547–560. [PubMed: 8714634]

Lai FM, Tanikella T, Cervoni P. Effect of gamma-aminobutyric acid (GABA) on vasodilation in resistance-sized arteries isolated from the monkey, rabbit, and rat. J Cardiovasc Pharmacol 1988;12:372–376. [PubMed: 2464112]

Leithner C, Royl G, Offenhauser N, Fuchtemeier M, Kohl-Bareis M, Villringer A, Dirnagl U, Lindauer U. Pharmacological uncoupling of activation induced increases in CBF and CMRO2. J Cereb Blood Flow Metab 2010;30:311–322. [PubMed: 19794398]

Li CL, Cullen C, Jasper HH. Laminar microelectrode studies of specific somatosensory cortical potentials. J Neurophysiol 1956;19:111–130. [PubMed: 13295835]

Logothetis NK, Wandell BA. Interpreting the BOLD signal. Annu Rev Physiol 2004;66:735–769. [PubMed: 14977420]

Martindale J, Berwick J, Martin C, Kong Y, Zheng Y, Mayhew J. Long duration stimuli and nonlinearities in the neural-haemodynamic coupling. J Cereb Blood Flow Metab 2005;25:651–661. [PubMed: 15703699]

Mathiesen C, Caesar K, Akgoren N, Lauritzen M. Modification of activity-dependent increases of cerebral blood flow by excitatory synaptic activity and spikes in rat cerebellar cortex. J Physiol 1998;512 (Pt 2):555–566. [PubMed: 9763643]

Mitzdorf U. Current source-density method and application in cat cerebral cortex: investigation of evoked potentials and EEG phenomena. Physiol Rev 1985;65:37–100. [PubMed: 3880898]

Ngai AC, Meno JR, Jolley MA, Winn HR. Suppression of somatosensory evoked potentials by nitric oxide synthase inhibition in rats: methodological differences. Neurosci Lett 1998;245:171–174. [PubMed: 9605483]

Norup Nielsen A, Lauritzen M. Coupling and uncoupling of activity-dependent increases of neuronal activity and blood flow in rat somatosensory cortex. J Physiol 2001;533:773–785. [PubMed: 11410634]

Rauch A, Rainer G, Logothetis NK. The effect of a serotonin-induced dissociation between spiking and perisynaptic activity on BOLD functional MRI. Proc Natl Acad Sci U S A 2008;105:6759–6764. [PubMed: 18456837]

Roberts F, Pearce M, Taberner PV. A comparison of the in vivo uptake of [3H]GABA into rat celebral cortex and dorsal medulla following topical application. Brain Res 1980;201:431–435. [PubMed: 7417852]

Roche-Labarbe N, Carp SA, Surova A, Patel M, Boas DA, Grant PE, Franceschini MA. Noninvasive optical measures of CBV, StO(2), CBF index, and rCMRO(2) in human premature neonates' brains in the first six weeks of life. Hum Brain Mapp 2010;31:341–352. [PubMed: 19650140]

Roy, N.; Contreras, D. The subcortical origin of multiwhisker receptive fields in layer 4 of barrel cortex and their modulation by anesthesia level. Neuroscience Meeting. Society for Neuroscience; San Diego, CA. 2007.

Sheth SA, Nemoto M, Guiou M, Walker M, Pouratian N, Toga AW. Linear and nonlinear relationships between neuronal activity, oxygen metabolism, and hemodynamic responses. Neuron 2004;42:347–355. [PubMed: 15091348]

Shi Y, Liu X, Gebremedhin D, Falck JR, Harder DR, Koehler RC. Interaction of mechanisms involving epoxyeicosatrienoic acids, adenosine receptors, and metabotropic glutamate receptors in neurovascular coupling in rat whisker barrel cortex. J Cereb Blood Flow Metab 2008;28:111–125. [PubMed: 17519974]

Siegel AM, Culver JP, Mandeville JB, Boas DA. Temporal comparison of functional brain imaging with diffuse optical tomography and fMRI during rat forepaw stimulation. Phys Med Biol 2003;48:1391–1403. [PubMed: 12812454]

Silva AC, Koretsky AP. Laminar specificity of functional MRI onset times during somatosensory stimulation in rat. Proc Natl Acad Sci U S A 2002;99:15182–15187. [PubMed: 12407177]

Simons DJ. Response properties of vibrissa units in rat SI somatosensory neocortex. J Neurophysiol 1978;41:798–820. [PubMed: 660231]

Staba RJ, Bergmann PC, Barth DS. Dissociation of slow waves and fast oscillations above 200 Hz during GABA application in rat somatosensory cortex. J Physiol 2004;561:205–214. [PubMed: 15550468]

Steriade, M. The excitatory-inhibitory response sequence in thalamic and neocortical cells: state-related changes and regulatory systems. In: Edelman, GMGW.; Cohen, WM., editors. Dynamic Aspects of Neocortical Function. John Wiley & Sons; New York: 1984. p. 107-158.

Strangman G, Culver JP, Thompson JH, Boas DA. A quantitative comparison of simultaneous BOLD fMRI and NIRS recordings during functional brain activation. NeuroImage 2002;17:719–731. [PubMed: 12377147]

Toronov V, Webb A, Choi JH, Wolf M, Michalos A, Gratton E, Hueber D. Investigation of human brain hemodynamics by simultaneous near-infrared spectroscopy and functional magnetic resonance imaging. Med Phys 2001;28:521–527. [PubMed: 11339749]

Ureshi M, Matsuura T, Kanno I. Stimulus frequency dependence of the linear relationship between local cerebral blood flow and field potential evoked by activation of rat somatosensory cortex. Neurosci Res 2004;48:147–153. [PubMed: 14741389]

Villringer A, Planck J, Hock C, Schleinkofer L, Dirnagl U. Near infrared spectroscopy (NIRS): a new tool to study hemodynamic changes during activation of brain function in human adults. Neuroscience Letters 1993;154:101–104. [PubMed: 8361619]

Viswanathan A, Freeman RD. Neurometabolic coupling in cerebral cortex reflects synaptic more than spiking activity. Nat Neurosci 2007;10:1308–1312. [PubMed: 17828254]

Wrobel A, Kublik E, Musial P. Gating of the sensory activity within barrel cortex of the awake rat. Exp Brain Res 1998;123:117–123. [PubMed: 9835400]

Yu G, Durduran T, Lech G, Zhou C, Chance B, Mohler ER 3rd, Yodh AG. Time-dependent blood flow and oxygenation in human skeletal muscles measured with noninvasive near-infrared diffuse optical spectroscopies. J Biomed Opt 2005;10:024027. [PubMed: 15910100]
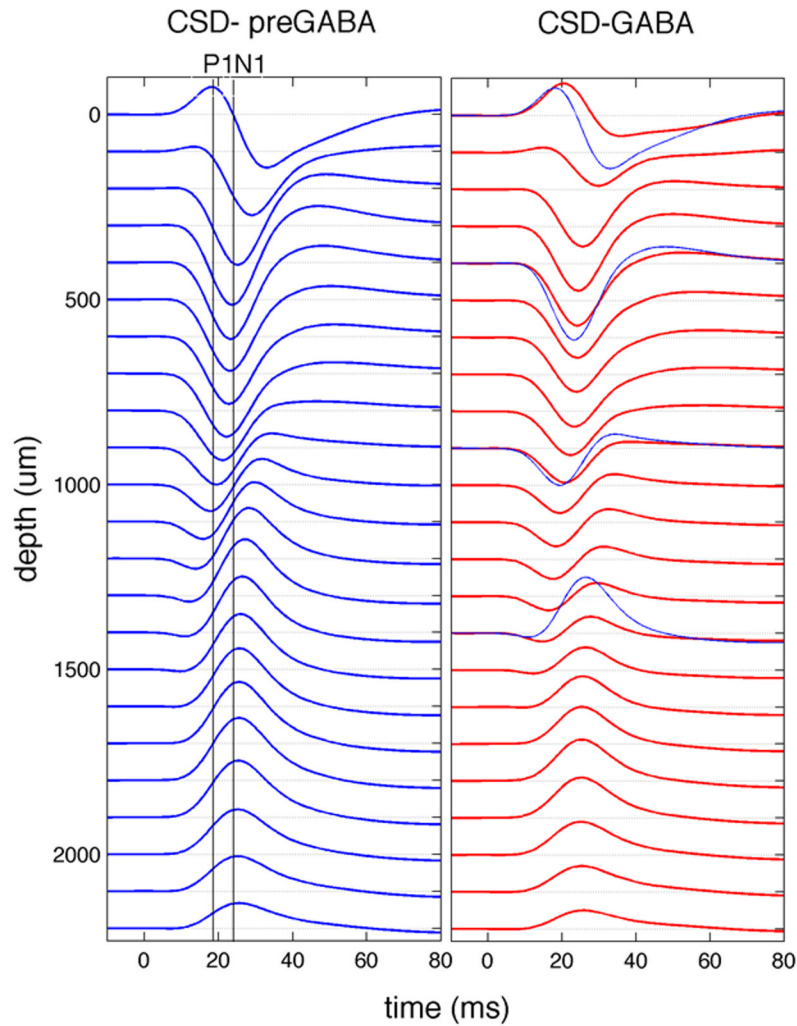
Fig. 1.
Current source density profiles in a representative animal. The traces shown are from before (left panel) and after (right panel) GABA application. The two vertical lines in the left panel show the times of initial sink at ~900 um and the secondary sink in the supragranular layers, corresponding to the peaks of P1 and N1 SEP components on the surface (see Figs. 3 and 4). After GABA application the secondary sink is reduced, while the initial sink is preserved. For better comparison in the right panel few pre-GABA CSD profiles are shown in blue together with the profiles during GABA (red). Stimulation occurred at t=0 ms. The responses from the surface are in the top 100 microns, the supragranular layers at depths of 200–400 microns, layer IV at 600–900 microns, and infragranular layers at 1300–1600 microns.
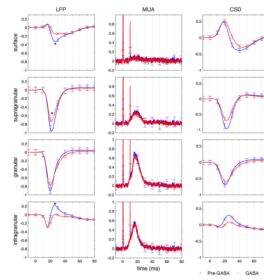
Fig. 2.
Average responses across the cortical column measured with a laminar electrode. Local field potential (left), multi-unit activity (middle) and current source density profiles (right) are obtained averaging across rats the electrodes on the surface (0–100 um depth, top panel), in superficial layers (200–400 um depth, supragranular), in the middle layer (600–900 um depth, granular), and in the bottom layers (1300–1600 um depth, infragranular). Blue traces correspond to pre-GABA responses and red traces to responses after GABA application. Error bars represent standard errors. Stimulation occurred at t=0 ms. * in the LFP graphs indicate statistically significant change (p-value<0.05) on the peak amplitude between the pre-GABA and GABA conditions.
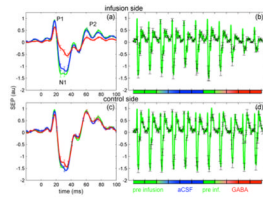
Fig. 3.
Grand average of contralateral SEP responses on the infusion (panels a and b) and control sides (panels c and d). Panels a and c: averages during pre-infusion (green), aCSF (blue) and GABA (red) cycles. Stimulation occurred at t=0 ms. Panels b and d: mean responses for each cycle. The SEP signals in each panel are normalized with respect to the maximum amplitude of P1.
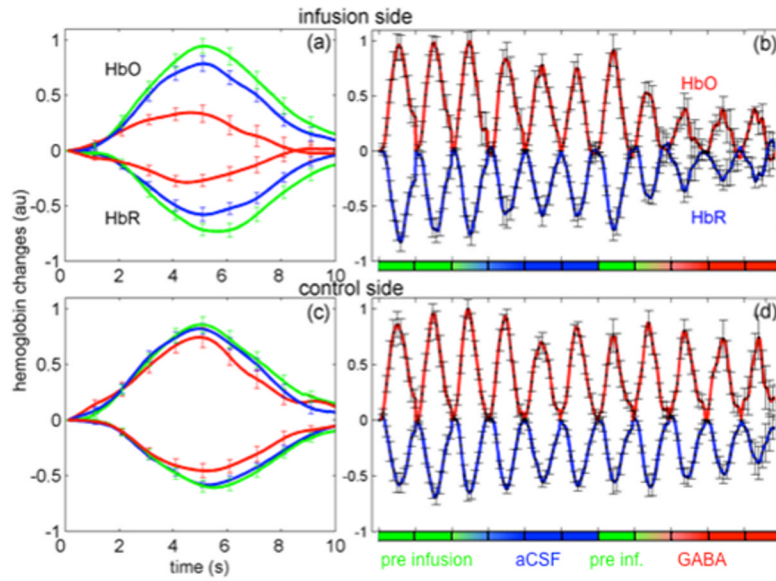
Fig. 4.
Grand average of contralateral hemoglobin responses on the infusion (panels a and b) and control sides (panels c and d). Panels a and c: averages during pre-infusion (green), aCSF (blue) and GABA (red) cycles. Stimulation occurred from t=0 to t=4 s. Panels b and d: mean responses for each cycle. HbO = positive changes, HbR = negative changes. The HbO and HbR in each panel are normalized with respect to the maximum amplitude of HbO.
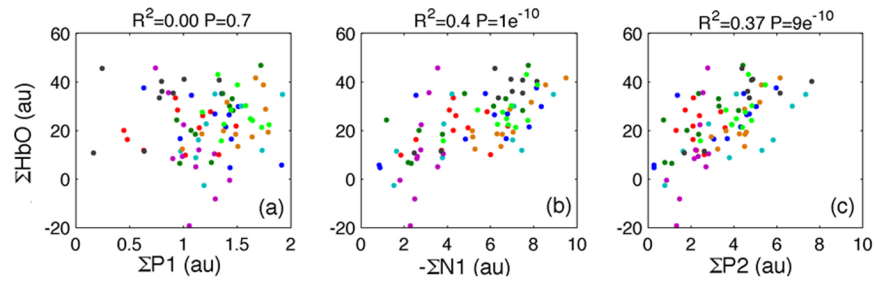
Fig. 5.
Scatter plots oxy-hemoglobin concentration and SEP components (P1, N1 and P2) for each cycle and each rat (shown with different colors) in the infusion side using area under the response. For each animal, the SEP and hemoglobin responses are normalized with respect to the peak amplitude of P1 and HbO during the pre-infusion cycles. Despite the variability of the SEP and hemodynamic responses between rats, there is a good correlation and high statistical significance between the hemoglobin and N1 and P2 responses (coefficient of determination R2 and p-values shown in each panel). The correlation between hemoglobin response and P1 is instead very low. Similar results, not shown, were obtained for deoxy-hemoglobin concentration.
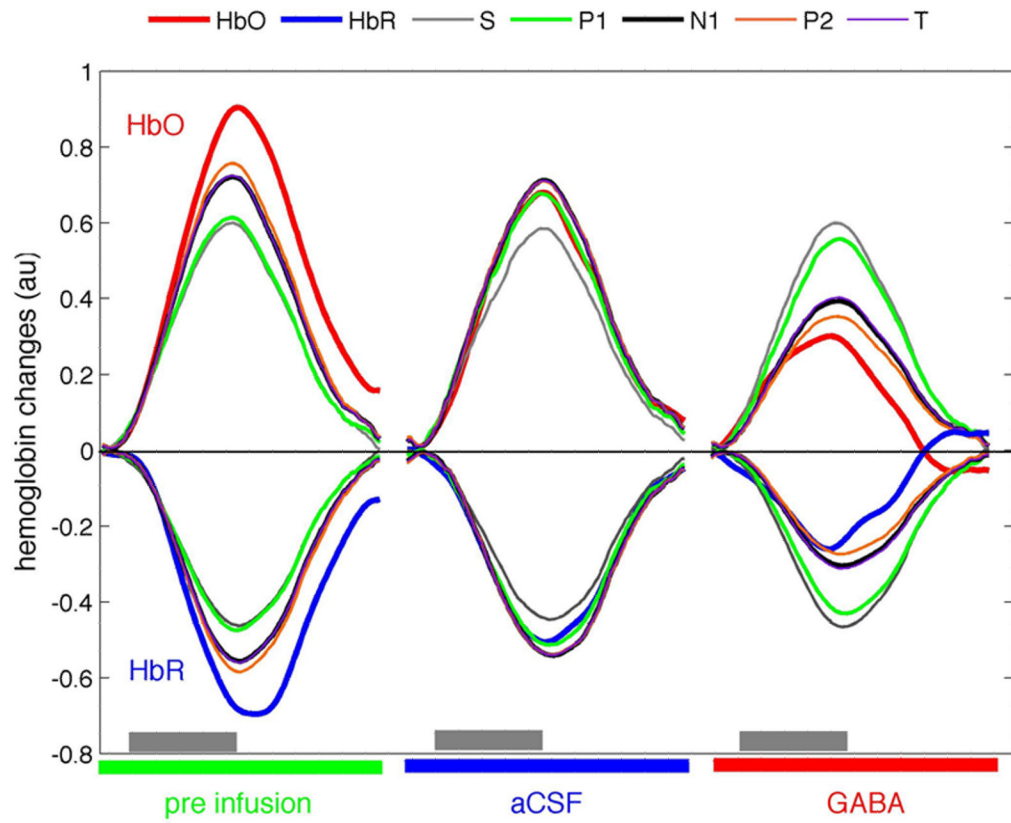
Fig. 6.
Grand average of the measured oxy-hemoglobin (red) and deoxy-hemoglobin (blue) responses to right forepaw stimulation in the infusion side during pre-infusion, aCSF and GABA conditions. Corresponding predictions of Hbo and HbR using the input stimuli (S, gray), area under the SEP components P1 (green), N1 (black), P2 (orange), and the total SEP response (T, purple) are shown in the figure. Gray bars indicate stimulation period.
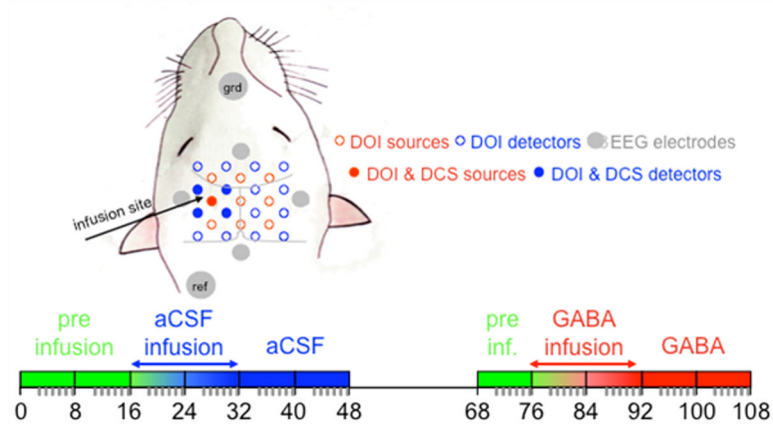
Fig. 7.
Schematic drawing of the optical probe and EEG electrode as positioned on the animal head (top) and schematic diagram of the experimental protocol (bottom). In all animals the infusion side was in the left hemisphere. The right and left forepaw were stimulated in sequence, while DOI and EEG data where acquired in both infusion and control sides for the entire time. The 11 blocks represent the 11 measurement cycles. During each cycle we acquired: 2 min of DCS during rest, 4 min of DOI and EEG during stimulation of the forepaw contralateral to the infusion side, and 2 min of DOI and EEG during stimulation of the forepaw contralateral to the control side. Green indicates pre-infusion cycles, blue aCSF cycles, and red GABA cycles. Between the aCSF and GABA cycles we waited 20 min to rest the animal.

Table 1

Average percent changes and standard errors of the SEP and hemoglobin concentration areas (top) and peak amplitudes (bottom) with respect to pre-infusion cycles. Positive changes indicate increase, negative decrease of the responses with respect to the pre-infusion cycles. Statistically significant changes are indicated in bold. Superscript numbers are the corresponding p-values.

	infusion side					control side				
	ΣP1	ΣN1	ΣP2	ΣHbO	ΣHbR	ΣP1	ΣN1	ΣP2	ΣHbO	ΣHbR
aCSF	$7\pm5^{.23}$	$-9\pm4^{.08}$	**$-16\pm5^{.03}$**	$-20\pm11^{.11}$	$-22\pm10^{.06}$	$-6\pm5^{.27}$	$-3\pm3^{.41}$	$-8\pm3^{.11}$	$-8\pm11^{.55}$	$-4\pm10^{.74}$
GABA	$-7\pm9^{.46}$	**$-50\pm7^{.000}$**	**$-59\pm7^{.001}$**	**$-66\pm13^{.002}$**	**$-65\pm12^{.002}$**	**$-27\pm8^{.03}$**	$-22\pm9^{.07}$	$-21\pm12^{.16}$	$-14\pm11^{.25}$	$-17\pm9^{.12}$

	infusion side					control side				
	P1	N1	P2	HbO	HbR	P1	N1	P2	HbO	HbR
aCSF	$-1\pm3^{.53}$	$-7\pm4^{.07}$	$-7\pm5^{.13}$	$-12\pm8^{.14}$	**$-18\pm7^{.03}$**	$-4\pm4^{.25}$	$-2\pm2^{.23}$	$-5\pm4^{.16}$	$-4\pm8^{.43}$	$-1\pm7^{.61}$
GABA	**$-28\pm6^{.001}$**	**$-41\pm6^{.000}$**	**$-41\pm6^{.000}$**	**$-37\pm6^{.000}$**	**$-41\pm7^{.000}$**	**$-21\pm6^{.007}$**	$-16\pm8^{.06}$	$-13\pm8^{.12}$	$-5\pm7^{.37}$	$-11\pm5^{.06}$